



Airborne and laboratory studies of an IAGOS instrumentation package containing a modified CAPS particle extinction monitor

Julia Perim de Faria, Ulrich Bundke, Marcel Berg, Andrew Freedman, Timothy B. Onasch & Andreas Petzold

To cite this article: Julia Perim de Faria, Ulrich Bundke, Marcel Berg, Andrew Freedman, Timothy B. Onasch & Andreas Petzold (2017) Airborne and laboratory studies of an IAGOS instrumentation package containing a modified CAPS particle extinction monitor, *Aerosol Science and Technology*, 51:11, 1240-1253, DOI: [10.1080/02786826.2017.1355547](https://doi.org/10.1080/02786826.2017.1355547)

To link to this article: <https://doi.org/10.1080/02786826.2017.1355547>



© 2017 The Author(s). Published with license by American Association for Aerosol Research© Julia Perim de Faria, Ulrich Bundke, Marcel Berg, Andrew Freedman, Timothy B. Onasch, and Andreas Petzold



Published online: 29 Sep 2017.



Submit your article to this journal [↗](#)



Article views: 706



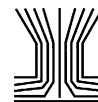
View related articles [↗](#)




View Crossmark data [↗](#)



Citing articles: 5 View citing articles [↗](#)



Airborne and laboratory studies of an IAGOS instrumentation package containing a modified CAPS particle extinction monitor

Julia Perim de Faria ^a, Ulrich Bundke ^a, Marcel Berg^a, Andrew Freedman ^b, Timothy B. Onasch ^b, and Andreas Petzold ^a

^aForschungszentrum Jülich GmbH, Institute of Energy and Climate Research, Jülich, Germany; ^bAerodyne Research Inc., Billerica, Massachusetts, USA

ABSTRACT

An evaluation of the operation and performance of a Cavity Attenuated Phase-Shift Particle Extinction Monitor (CAPS PM_{ex}) was performed for use on board commercial aircraft as part of the research infrastructure IAGOS (In-service Aircraft for a Global Observing System, www.iagos.org). After extensive laboratory testing, a new flow system, using mass flow controllers, was installed to maintain constant purge and sample flows under low and varying pressure conditions. The instrument was then tested for pressures as low as 200 hPa and evaluated against particle-free compressed air and CO₂. Extinction coefficients for the studied gases were in close agreement with literature values with differences between 2.2% and 8%, proving that the CAPS technology works at low pressures. The instrument's limit of detection, with respect to 3 times the variability of the background signal for the full pressure range, was 0.2 Mm⁻¹ for 60s integration time. During its first research aircraft operations, the IAGOS instrument prototype, composed of one CAPS PM_{ex} and one OPC, showed excellent results regarding the stability of the instruments and the potential for characterizing different aerosol types and for estimating the contribution of sub- and super- μ m sized particles to aerosol light extinction.

ARTICLE HISTORY

Received 16 December 2016
Accepted 26 May 2017

EDITOR



Thomas Kirchstetter

Introduction

The impact of atmospheric aerosol particles (hereafter called “aerosols”) on atmospheric radiation properties and climate has been a topic of extensive research for many years (Boucher et al. 2013). They affect the radiation balance of the Earth through scattering and absorbing the incoming solar radiation, also called the aerosol direct effect. Compared to greenhouse gases, aerosols are characterized by a shorter residence time in the atmosphere and have highly variable chemical compositions and sizes. Their distribution is heterogeneous both spatially and seasonally in most cases. Therefore, understanding the impacts of aerosols on the atmosphere and climate on a global scale requires knowledge on both the small-scale microphysical processes and the large-scale dynamical processes (Boucher et al. 2013). According to Haywood and Shine (1995) and McComiskey et al. (2008), the aerosol driven radiative forcing depends on three main parameters: aerosol optical

depth (AOD) – a measure of the extinction of the solar light by aerosols integrated over a certain column; single-scattering albedo (SSA) – the relation between the scattering and the extinction of light by aerosols; and the hemispheric upscatter fraction – the fraction of radiation scattered in the upward direction by aerosols. Thus, for quantifying the change of the Earth's energy balance caused by aerosols, the continuous global-scale monitoring of AOD and vertical profiles of the extinction coefficient are of high priority, but still represent a challenge.

Many initiatives such as the Aerosols, Clouds, and Trace gases Research Infrastructure Network (ACTRIS) (Pappalardo et al. 2014) and the Aerosol Robotic Network (AERONET) (Holben et al. 1998; Holben et al. 2001) have been launched in the past to measure the AOD and aerosol vertical profiles by using remote-sensing technologies, enabling the quantification of the direct impact of aerosols on climate. These very successful projects operate

CONTACT Ulrich Bundke  u.bundke@fz-juelich.de  Forschungszentrum Jülich GmbH, Institute of Energy and Climate Research 8: Troposphere, 52425 Jülich, Germany.

Color versions of one or more of the figures in the article can be found online at www.tandfonline.com/uast.

© Julia Perim de Faria, Ulrich Bundke, Marcel Berg, Andrew Freedman, Timothy B. Onasch, and Andreas Petzold

This is an Open Access article distributed under the terms of the Creative Commons Attribution-NonCommercial-NoDerivatives License (<http://creativecommons.org/licenses/by-nc-nd/4.0/>), which permits non-commercial re-use, distribution, and reproduction in any medium, provided the original work is properly cited, and is not altered, transformed, or built upon in any way.

Published with license by American Association for Aerosol Research

remote-sensing ground-based techniques, such as Light Detection and Ranging (LIDAR) and Sun Photometers. However, the measurement errors depend on weather conditions (optimum operation condition with clear sky) and may fail in the retrievals of aerosol intensive properties when found in lower concentrations (Petzold et al. 2013a; Sheridan et al. 2012). In addition, the aerosol optical depth is measured globally by satellite-based remote sensing instruments using specialized technologies, e.g., MODIS (Moderate-resolution Imaging Spectroradiometer), which complement the previously mentioned ground-based methods (Anderson et al. 2005). This well-established network provides a very good global-scale mapping of the AOD, but it encounters several problems: (a) lack of standardized calibration method for the different satellite-based instruments; (b) different sampling and cloud screening algorithms; (c) variable treatment of the surface reflectivity; and (d) low accuracy of derived aerosol microphysical properties (Myhre et al. 2013). The major limitation of this integrated AOD observing system, composed of the space component and ground-based networks such as ACTRIS and AERONET, is the lack of an in situ measurement component for column-based measurement validation.

To validate both forecast models and remote sensing methods, vertical profiles of in situ aerosol optical properties have been measured extensively by research aircraft (Petzold et al. 2002; Schmid et al. 2006; Sheridan et al. 2012; Weinzierl et al. 2009). Schmid et al. (2006) have evaluated the state of the art technologies for the in situ measurement of aerosol extinction coefficients onboard research aircraft: the airborne sun photometer (AATS-14), an airborne nephelometer plus particle soot absorption photometer combination, and an airborne cavity ring-down system (CRD). The study shows that the CRD and the nephelometer plus absorption photometer agree well, with about 5% difference for in situ extinction coefficient values. In comparison to the derived extinction coefficient from AATS-14, the extinction coefficient measured by CRD and the nephelometer plus absorption photometer express lower values, with a difference of 7–14% for visible light and 40% in the near infrared spectrum. According to the authors, this low bias of the in situ measurement with respect to AATS-14 is due to a combination of uncorrected effects of the evaporation of water, organics or nitrates, and sampling losses to the in situ data. Of these methods, the CRD technique is the only one that provides in situ aerosol extinction coefficient measurements. It has provided very good results in previous studies (Moosmüller et al. 2005; Strawa et al. 2003); however, the instrument is custom built which implies complexities using the system on airborne platforms.

An alternative technology, the Cavity Attenuated Phase Shift Particle Extinction Monitor (CAPS PM_{ex}), was commercially introduced in 2007 to directly measure the extinction of particles (Kebabian et al. 2007; Massoli et al. 2010). The instrument is available at several operation wavelengths in the visible range. In contrast to the deployment of a laser in the CDR, it uses light emitting diodes (LED) as a light source. The CAPS PM_{ex} can be readily applied in mobile sampling systems since it is compact and robust (Kebabian et al. 2007), with a relatively low-cost set up. The CAPS PM_{ex} operational principle has been successfully assessed in optical closure studies and deployed at ground pressure conditions with artificially generated and ambient aerosols (Massoli et al. 2010; Petzold et al. 2013b) and high concentration exhaust aerosols (Yu et al. 2011).

Our study aims to define the necessary modifications of the CAPS PM_{ex} system required for conditions relevant to operation on board passenger aircraft. This is the first step towards incorporating a CAPS PM_{ex} system into the instrumentation operated in the framework of the European Research Infrastructure IAGOS. This infrastructure aims at the in situ monitoring of atmospheric chemical composition, aerosols, and clouds through the installation of a high-technology measurement instrumentation system on board a globally operating fleet of commercial aircraft (Petzold et al. 2015). The CAPS PM_{ex} system is intended to be part of a new IAGOS instrument package focusing on the characterization and quantification of aerosol light extinction as one of the essential climate variables (Bojinski et al. 2014).

Instruments and methods

Throughout our study, we refer to extinction, scattering and absorption coefficients of gases and particles by σ_{eg} , σ_{sg} , σ_{ag} , and by σ_{ep} , σ_{sp} , σ_{ap} , respectively, to the Ångström exponent by α , and to optical cross sections by C .

CAPS PM_{ex} system

The CAPS PM_{ex} system uses a form of cavity enhanced spectroscopy to produce the long path length (2–3 km) needed to measure low values of particle extinction coefficients. Briefly, light from a square-wave modulated LED is focused into an optical cavity formed by two high reflectivity mirrors; the light that leaks out of the cell, passes through a 10 nm wide interference filter to reject light from wavelengths outside the reflectivity band of the mirrors, and is detected by a vacuum photodiode. The waveform that is measured is characterized by its phase shift with respect to the initial square wave which in turn is used to calculate the optical loss in the system.

The optical extinction coefficient of a sample of aerosol particles is determined by measuring the optical loss with and without particles in the sample cell.

The sample flow, controlled by a critical orifice at 0.85 lpm, continuously enters the sample cell, which consists of a 26 cm long near-confocal optical cavity of 2.0 cm inner diameter with high reflectivity mirrors of 60–70 ppm nominal transmission and radius curvature of 26 cm enclosing the chamber. To keep the mirrors clean, a combined purge flow of 25 cm³ min⁻¹ of particle-free air is continuously maintained. The modulation frequency is usually set to 17 kHz which provides an initial phase shift of 35–40° if the mirrors are clean. The time response of the monitor is 1–2 seconds and, according to Massoli et al. (2010) and Petzold et al. (2013b), its limit of detection (LOD = 3 σ where σ is the r.m.s. noise for particle-free air) ranges between 1–3 Mm⁻¹ (1 second sample period), depending on the particular instrument, and decreases as the square root of the sample period to at least 100 seconds. The monitor provides an absolute measurement without the need of further calibration.

In order to maintain an optimum operational performance, the equipment includes an automatic baseline measurement mechanism. Within a regular interval and duration set by the user, sample air is routed through a particle-filter using a computer controlled 3-way ball valve and flushes the sample cavity with particle-free air to obtain the baseline which comprises the Rayleigh scattering (and any absorption) of gases present in the cell and any losses by degraded mirrors. Effects of changes in pressure and temperature on the gas Rayleigh scattering coefficient in the cell compared to the baseline period are taken into account by a correction algorithm based on the ideal gas law. The residence time of the sample inside the measurement cell ensures the

equilibrium of sample and cell temperatures (Kebabian et al. 2007). The CAPS PM_{ex} system used in this study operates at a wavelength of 630 nm and thus shows minimal interference with absorbing gaseous species such as nitrogen dioxide; a NO₂ volume mixing ratio of 1 ppb produces an extinction coefficient of 0.04 Mm⁻¹ at the operation wavelength.

Laboratory study

The laboratory study was conceived to evaluate the operational principle of the CAPS PM_{ex} and its performance and accuracy when measuring at low pressure conditions. As stated before, the technology has already been assessed both using optical closure approaches and in comparison with Mie theory (Massoli et al. 2010; Petzold et al. 2013b). While all previous studies were performed at ground pressure, the operation on board aircraft requires a feasibility study at low pressure. For this purpose, the system was tested with particle-free compressed air and carbon dioxide gas (CO₂). For the CO₂ experiment, the system was filled with 99.995% purity CO₂ at ground pressure of approx. 970 hPa and a baseline was taken. Then, the cavity was slowly evacuated down to a pressure of 200 hPa with steps of 50 hPa and the relative changes of the Rayleigh scattering coefficient of the gas were recorded as function of cell pressure. Upstream of the cavity, a HEPA capsule (99.97% retention of 0.3 μ m aerosol) and a condensation particle counter (CPC) were placed to ensure that particle-free gas was entering the system; Figure 1. for details.

To analyze the instrument noise/residuum and operability of the instrument at the different pressure levels, the observed extinction coefficients, which correspond to the Rayleigh scattering coefficients of the studied gases

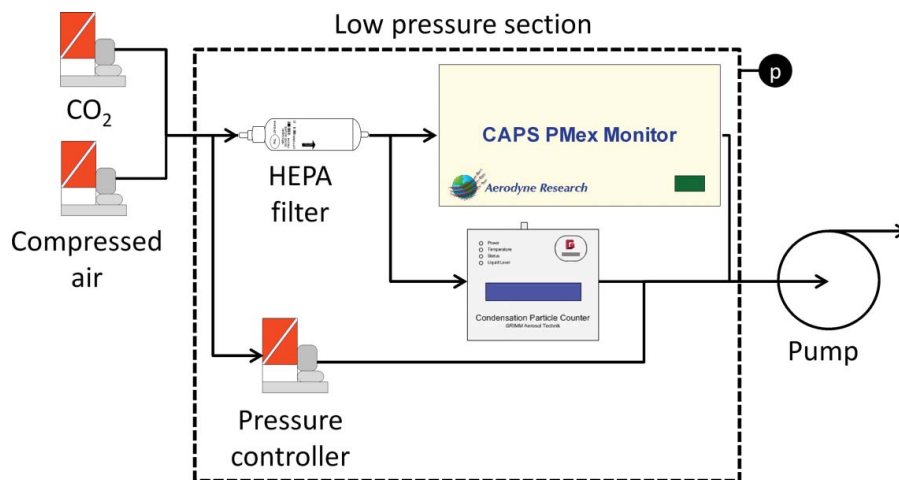


Figure 1. Experimental set-up of the laboratory work.

(particle-free air and CO₂), were compared to theoretically expected values. The theoretically expected scattering coefficients were calculated as follows: first, the initially measured extinction coefficient was adjusted for STP conditions (standard temperature 273.15 K and pressure 1013.25 hPa) and set as the reference value; then, for each pressure level, the expected extinction coefficient was calculated from the initial STP reference point for the actual pressure and temperature values (p, T) by calculating the molecular number density N (p, T) in accordance to the ideal gas law and applying it to Equation (1)

$$\sigma_{sg}(p, T) = C_{sg} \cdot N(p, T) \cdot \lambda^{-4} \quad [1]$$

where σ_{sg} is the Rayleigh scattering coefficient of the gas molecules, C_{sg} is the scattering cross-section of the gas molecules and N is the molecular number density. Knowing that particle-free air and gas phase CO₂ do not absorb at 630 nm, we equate the theoretically expected $\sigma_{sg}(p, T)$ values with $\sigma_{eg}(p, T)$ values and use these as the reference case. The residual analysis was done by subtracting the measured values from the corresponding reference $\sigma_{eg}(p, T)$ values for 1 and 60 seconds integration times.

We also compared the measured extinction coefficients to literature data by Cutten (1974), Bodhaine et al. (1991), Anderson et al. (1996), Bodhaine et al. (1999) and Sneep and Ubachs (2005). The dependence between the Rayleigh extinction/scattering coefficient and the wavelength is governed by the extinction Ångström exponent of the gas. Cutten (1974), Bodhaine et al. (1991), and Anderson et al. (1996) report the Rayleigh scattering coefficient for CO₂ for at least 3 wavelengths, but not for the operation wavelength of the CAPS PM_{ex} of 630 nm. To derive the value of σ_{eg} at 630 nm, the extinction Ångström exponent (α_{eg}) was calculated using the given values for blue, from 450 to 495 nm (λ_1), and red, from 620 to 750 nm (λ_2), wavelengths as shown in Equation (2). From the calculated α_{eg} , the value of σ_{eg} (STP) for CO₂ at 630 nm (λ_3) was calculated via Equation (3).

$$\alpha_{eg} = \frac{-\ln(\sigma_{eg\lambda_1} / \sigma_{eg\lambda_2})}{\ln(\lambda_1 / \lambda_2)} \quad [2]$$

$$\frac{\sigma_{eg\lambda_3}}{\sigma_{eg\lambda_1}} = \left(\frac{\lambda_3}{\lambda_1}\right)^{-\alpha_{eg}} \quad [3]$$

To compare to the reference given by Bodhaine et al. (1999), Equations (4) and (5) were used

$$C_{sg} = \frac{24\pi^3 (m_g(\lambda_3)^2 - 1)^2}{\lambda_3^4 N_s^2 (m_g(\lambda_3)^{22} + 2)} * 1.15 \quad [4]$$

with

$$\begin{aligned} & (m_{CO_2}(\lambda_3) - 1) * 10^8 \\ & = 22822.1 + 117.8\lambda_3^{-2} + \frac{2406030}{130 - \lambda_3^{-2}} + \frac{15997}{38.9 - \lambda_3^{-2}} \end{aligned} \quad [5]$$

where C_{sg} is the scattering cross-section of the gas molecule in cm², m_g is the index of refraction of the gas, λ is the wavelength, and N_s is the number of molecules per cm³. The factor 1.15 in Equation (4) is the King factor $F_k(\lambda)$ (Bodhaine et al. 1999); and m_{CO_2} is the index of refraction of CO₂. The value of C_{sg} from Equation (4) was then inserted into Equation (1) to calculate the reference $\sigma_{sg} = \sigma_{eg}$. Finally, the measured and the reference values were compared using linear regression analysis.

All σ_{sg} values for CO₂ from literature were combined and α_{s,CO_2} was determined by curve fitting. The same procedure was applied to particle-free compressed air using the references given by from Cutten (1974), Bodhaine et al. (1991), Anderson et al. (1996) and Thalman et al. (2014).

Airborne test campaign

The Baltic Sea Experiment (BALTEX) in the summer 2015 was used as an opportunity to operate the instrument prototype on a research aircraft. The experiment itself aimed at the measurement and characterization of the emission plume of a specific ship during its cruise through the Baltic Sea from Helsinki (Finland) to Kiel via Gdynia (Poland). The research equipment was installed on board the research aircraft Polar 6 of type Basler BT-67, operated by the Alfred-Wegener-Institute (AWI). The campaign was a joint effort between several German research institutions and universities, and coordinated by AWI.

For the operation on board aircraft, the CAPS PM_{ex} system was dismantled and remounted in an IAGOS type instrument frame together with an optical particle counter (OPC - GRIMM Model 1.129, operating at 655 nm). We refer to this instrument as the IAGOS prototype instrument. During in-flight operation, a baseline was taken every 20 minutes with a duration of 45 seconds followed by a 28 seconds flushing period. No baselines were taken during aircraft vertical operations (e.g., ascent or descent). This new IAGOS prototype instrument is designed for measuring the volume aerosol extinction coefficient (σ_{ep} (630 nm))

together with the aerosol number concentration for particles with diameters $d_p > 250$ nm (N_{250}) and size distributions obtained by the OPC for particles between 0.25 and 3 μm in diameter. Combining these observation parameters and applying Mie theory to the measured size distribution, we expect to quantify the contribution of sub- μm and super- μm sized particles to aerosol light extinction.

In addition to the IAGOS prototype instrument, the BALTEX scientific payload included another IAGOS aerosol instrument which was composed of one OPC of type GRIMM Model 1.129, one CPC of type GRIMM Model 5.411 and a second CPC of the same type, connected to a thermodenuder (TDN) set to 250°C (Bundke et al. 2015).

The research aircraft performed 6 flights during the BALTEX campaign for a total of 20 flight hours. For this work, the two ferry flights were selected: the ferry flight to Bornholm, Denmark, on 20th August, to assess the operational behavior of the instrument in a very clean atmosphere with $N_{250} < 2$ cm^{-3} at cruise altitude, and the flight from Bornholm, Denmark to Bremerhaven, Germany, on 30th August, for presenting the most diverse atmospheric conditions (maritime and continental air masses at different altitudes).

Results and discussion

In this section, we present the results and relevant discussions of findings for the laboratory experiments, including the necessary modifications of the CAPS PM_{ex} ,

and the evaluation of the instrument operation under airborne conditions, including a noise analysis comparison between airborne and laboratory operations.

CAPS PM_{ex} evaluation and system modifications

During initial low pressure tests with the original equipment, we noticed that the internal flows (both purge and sample flows) were not constant through the low pressure operation. An increase in the purge flow and a decrease in the sample flow were observed as the critical orifices regulating sample and purge flow were no longer being operated under choked flow conditions because of the limitation of the supplied diaphragm pump. This could lead to errors in the measurement due to variable sample dilution and/or a reduction of the effective path length. To have a reliable operation of the system on board aircraft, a stable and robust flow regulation system is necessary.

Flow stabilization was achieved by substituting the critical orifices of the CAPS PM_{ex} with two mass flow controllers (MFCs) operated for constant volumetric flow, one with a nominal maximum flow of 3 lpm for the sample line, and the other with a nominal maximum flow of 0.5 lpm for the purge line. We preferred MFCs instead of a stronger vacuum unit to gain flexibility in the adjustment of purge and sample flows. The modification of the flow system is shown in Figure 2. Through LABVIEW™, the desired volumetric flows for the purge and sample lines were set and kept constant for pressure conditions encountered during operation. A zero particle filter was added as buffer volume to the

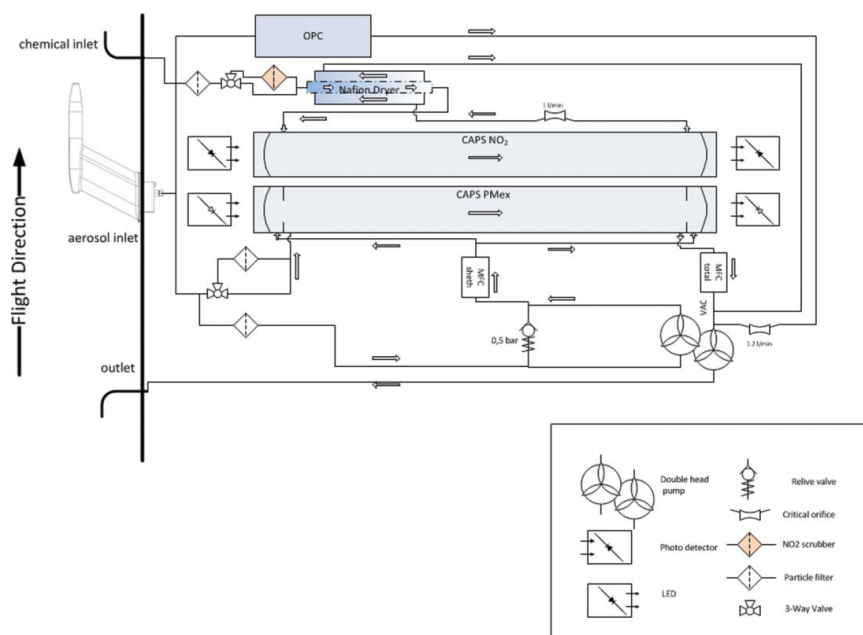


Figure 2. CAPS PM_{ex} internal flow modification: Plumbing Plan of the IAGOS compatible prototype combining CAPS PM_{ex} , OPC and CAPS NO_2 .

system upstream of the pump to reduce the fluctuations driven by the vacuum unit.

A second modification of the original system is associated with an observed temperature dependence of the instrument response (not shown). To assess the stability of the instrument over a long-term unassisted operation, the CAPS PM_{ex} was operated with particle-free air at ambient conditions for 160 h. The data analysis of the measured values showed a correlation between the signal and the temperature of the system, which is accounted for under normal baseline operations. However, this is critical when operating the equipment on board aircraft in an environment with significant temperature fluctuations occurring at a higher frequency than baselines can be obtained. For further tests, a temperature stabilization of the measurement system at 45°C, was applied (shown in Figure 2). Similar to the CAPS NO_2 setup, the temperature controller driven power resistors were mounted on the optical baseplate. The optical system is entirely housed to avoid convective heat transfer. This solution is only applied to the optical system (measurement chamber). The other parts are, in contrast, ventilated to reduce the heat load of electronic components. This implies that the measured aerosol is at much lower relative humidity than the aerosol at ambient conditions outside the aircraft.

Figure 3 show the 3-D drawing of the final IAGOS instrument prototype with all components fitted into the IAGOS instrument frame, including the temperature stabilization. The size of the frame is 560 mm × 400 mm × 296.5 mm and the total weight of the instrument is 30 kg.

Noise analysis

The original CAPS PM_{ex} instrument background noise was determined by means of an Allan variance analysis. This method was applied to the data set of 96 hours of operation at ambient conditions (temperature and pressure) with particle-free air. The running-average analysis for 1, 10, 60, and 100 seconds integration time for each specific operational pressure showed that the noise of the instrument does not depend on the operating pressure, and the instrument physical principle works at pressures as low as 200 hPa (correspondent to a flight altitude of approximately 12000 meter). The results are shown in Figure 4. Considering 1 second averaged data, the standard deviation is 0.274 Mm^{-1} and decreases to 0.046 Mm^{-1} for 60 seconds running averages. The Allan analysis is in accordance to what has been shown by Massoli et al. (2010) and Keabian et al. (2007) for CAPS systems operating at ambient pressure condition.

The potential disturbances caused by the modifications to the internal flow system were assessed by an Allan variance analysis. The new Allan deviation over time is also shown in Figure 4 for operation at different pressure levels together with the Allan analysis of the original setup using critical orifices. The initial value at ambient pressure with MFC installed (1 second measurement) is only 3.3% higher compared to 0.274 Mm^{-1} for the original setup with critical orifices. For 60 seconds integration time the measurement is 14% higher compared to 0.046 Mm^{-1} for the original system. The shift with integration time is caused by the addition of the

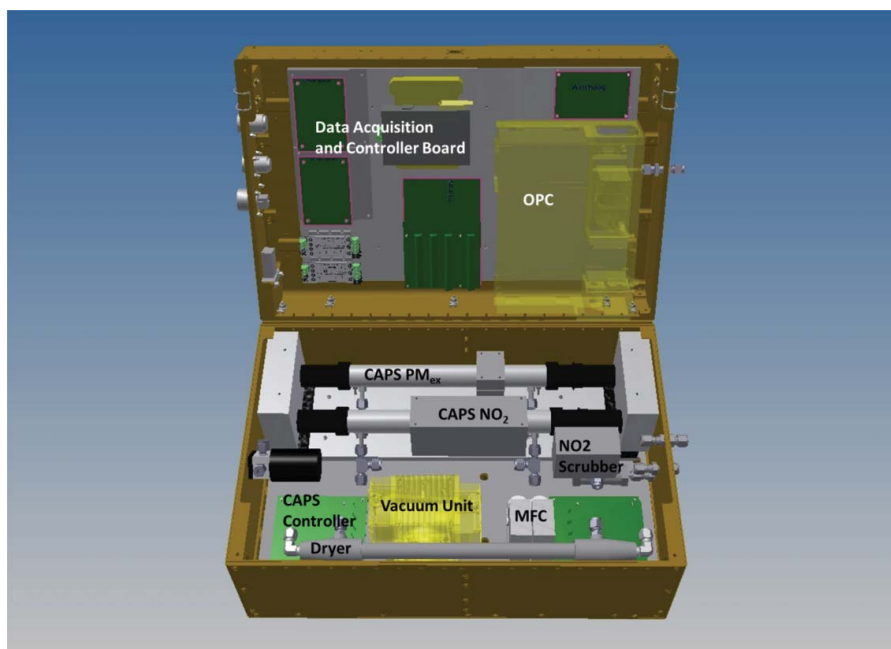


Figure 3. 3D drawing of IAGOS compatible frame prototype containing the CAPS PM_{ex} and OPC.

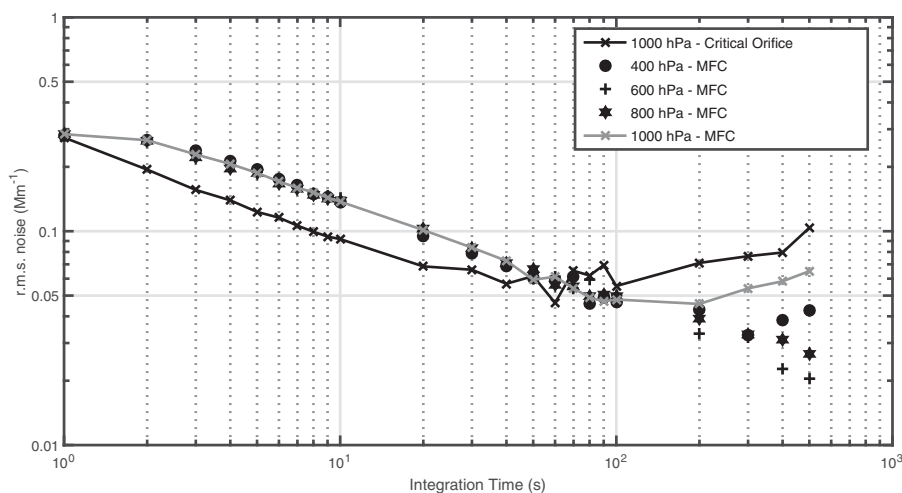


Figure 4. Allan standard deviation plot of the noise of the extinction coefficient at ambient pressure before and after flow modification at different pressures.

MFC's which are regulated by a proportional-integral-derivative controller (PID Controller) and adds thus a time dependent element to the regulation system, not present when using critical orifices.

The limit of detection (LOD) based on the “ 3σ ” criteria applied to the IAGOS CAPS PM_{ex} particle-free baseline for 96 hours of operation is 0.90 Mm^{-1} for an integration time of 1 second and 0.20 Mm^{-1} for 60 seconds integration time. These values are very close to the minimum extinction coefficients found by Petzold et al. (2002) for the upper troposphere (min. 0.10 and max. 1.10 Mm^{-1}) and free troposphere (min. 0.70 and max. 12 Mm^{-1}) over continental Europe, whereas respective values of desert regions are larger by one order of magnitude or more (Weinzierl et al. 2009). This comparison demonstrates that the equipment is suitable for measurements in the extratropical upper free troposphere, as envisaged by IAGOS.

CAPS PM_{ex} operation at low pressure – laboratory tests

The operation of CAPS PM_{ex} at low pressures was tested with CO_2 and particle-free air. The scatter plot of the measured CO_2 extinction coefficient and the calculated Rayleigh scattering coefficient for the reference case over the investigated pressure range is shown in Figure 5a. The extinction coefficient decreases with decreasing pressure in accordance with the ideal gas law. The measured values show a very good agreement with the reference values, with differences between 2.4% to the values derived from Cutten (1974) and 8% compared to the values derived from Bodhaine et al. (1991). The linear regression analysis results are shown in Table 1, whereas Table 2 shows the values from Cutten (1974), Bodhaine et al. (1991), and Anderson et al. (1996) for CO_2

Rayleigh scattering coefficients. Table 2 includes the Rayleigh scattering coefficient calculated by the power law fit using Equations (2) and (3) for the desired wavelength (630 nm), the calculated Rayleigh scattering coefficient using the methodology of Bodhaine et al. (1999), and the measured extinction coefficient by the CAPS PM_{ex} at a wavelength of 630 nm (values are in bold letters). Figure 5b shows the measured extinction and Rayleigh scattering coefficients from the referenced literature with the resulting power curve fit for the wavelength dependence inserted. The difference between the measured σ_{eg} and the σ_{sg} wavelength-adjusted by the power curve was 4.5%. This difference is comparable to the value of 5 to 9% found by Snee and Ubachs (2005) CRD technology operating at 532 nm.

The residual analysis (not shown) of the CO_2 scattering coefficient data shows a residuum for the 1 second averaging time data of the order of $\pm 0.50 \text{ Mm}^{-1}$ throughout the whole experiment pressure range from 1000 to 200 hPa. For the 60 seconds integration time case, the values are in the order of $\pm 0.20 \text{ Mm}^{-1}$. This result shows that the instrumental accuracy does not change over the investigated pressure range.

For the low pressure test performed with particle-free air, the linear regression analysis results are also shown in Table 1. The measured extinction coefficient shows a very good agreement with the reference values, between < 1% difference on the slope compared to the derived value from Thalman et al. (2014) and 5% compared to the derived using Anderson et al. (1996). Regarding the intercepts, all values are below 0.2 Mm^{-1} . Table 2 shows the values from Cutten (1974), Bodhaine et al. (1991), Anderson et al. (1996), and Thalman et al. (2014) for the Rayleigh scattering coefficient of particle-free air, including the Rayleigh scattering coefficient calculated by the power law fit using Equations (2) and (3) for the desired wavelength (630 nm), and the measured

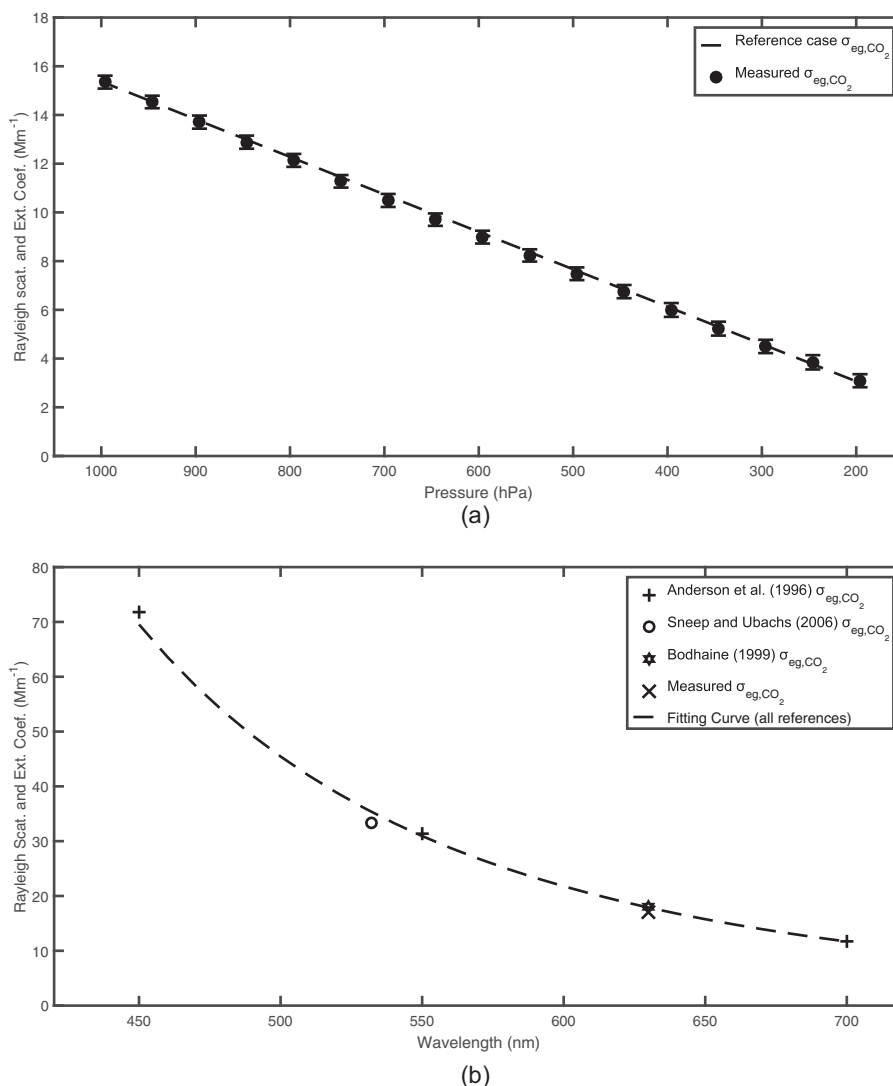


Figure 5. (a) Comparison of the measured CO_2 extinction coefficient values with the reference case. Here error bars represent the standard deviation of the measured variability including the error propagated instrumental precision (b) Literature and measured Rayleigh scattering and extinction coefficients for CO_2 at different wavelength.

extinction coefficient by the CAPS PM_{ex} . The results obtained for the CAPS PM_{ex} wavelength, 630 nm, are highlighted. The difference of the measured σ_{eg} from the σ_{sg} calculated with power curve fitting for all references was 3.2%. This confirms the previous finding, that the operation at low pressure is reliable and in accordance with theory and literature.

In-flight results

CAPS PM_{ex} in-flight performance assessment

During one flight sequence in the free-troposphere on 25 August, the IAGOS CAPS PM_{ex} sampled air with a very low aerosol load of less than 2 particles cm^{-3} on average in the detection size range of the optical particle counter

Table 1. Linear regression analysis results between the measured values, the reference case and the literature data ($y = ax + b$).

Author	CO_2 (n = 8042)					Air (n = 21796)				
	a	Std a	b	Std b	R^2	a	Std a	b	Std b	R^2
reference case	1.00	8.34E-4	0.08	0.01	0.99	1.00	1.03E-3	-0.16	0.01	0.96
Cutten (1974)	1.02	8.54E-4	0.08	0.01	0.99	0.96	1.03E-3	-0.15	0.01	0.96
Bodhaine et al. (1991)	1.08	9.00E-4	0.09	0.01	0.99	0.96	1.03E-3	-0.15	0.01	0.96
Anderson et al. (1996)	1.06	8.82E-4	0.08	0.01	0.99	0.95	1.03E-3	-0.15	0.01	0.96
Bodhaine et al. (1999)	1.05	8.79E-4	0.08	0.01	0.99	NA	NA	NA	NA	NA
Thalman et al. (2014)	NA	NA	NA	NA	NA	1.00	1.03E-3	-0.16	0.01	0.96

Table 2. Rayleigh scattering coefficient values from literature and measured by the CAPS PM_{ex} for CO₂ and air at STP.

Reference	Wavelength (nm)	Rayleigh Scat. Coef. (Mm ⁻¹) Air	Cross-Section Air (cm ²)	Rayleigh Scat. Coef. (Mm ⁻¹) CO ₂	Cross-Section CO ₂ (cm ²)
Cutten (1974)	460	25.5	9.5E-27	63.5	2.4E-26
	500	18.1	6.7E-27	45.1	1.7E-26
	550	12.3	4.6E-27	30.5	1.1E-26
	600	8.6	3.2E-27	21.4	8.0E-27
	630	7.1	2.6E-27	17.5	6.5E-27
Bodhaine et al. (1991)	450	27.9	1.0E-26	72.8	2.7E-26
	550	12.3	4.6E-27	32.0	1.2E-26
	630	7.1	2.6E-27	18.4	6.9E-27
	700	4.6	1.7E-27	12.0	4.4E-27
Anderson et al. (1996)	450	27.6	1.0E-26	71.8	2.7E-26
	550	12.1	4.5E-27	31.4	1.2E-26
	630	7.0	2.6E-27	18.0	6.7E-27
	700	4.5	1.7E-27	11.7	4.4E-27
Bodhaine et al. (1999)	630	NA	NA	18.0	6.7E-27
Sneep and Ubachs (2005)	532	NA	NA	33.3	1.2E-26
Thalman et al. (2014)	370	65.2	2.4E-26	NA	NA
	405.8	44.5	1.7E-26	NA	NA
	630	7.4	2.7E-27	NA	NA
	660	6.1	2.3E-27	NA	NA
Present Work	630	7.3	2.7E-27	17.1	6.4E-27

($d_p > 250$ nm) and about 680 particle cm^{-3} for the CPC detection size range ($d_p > 10$ nm). This data set was used to compare the background noise performance of the instrument for in-flight and laboratory conditions (800 hPa with particle free air). The IAGSO CAPS PM_{ex} reports background noise values for 1s integration time of $\sigma_{\text{ep,lab}} = 0.08 \pm 0.27$ Mm⁻¹ in the laboratory and $\sigma_{\text{ep,flight}} = -0.10 \pm 0.60$ Mm⁻¹ during flight operation; values for 10 s integration time are $\sigma_{\text{ep,lab}} = 0.08 \pm 0.07$ Mm⁻¹ and $\sigma_{\text{ep,flight}} = -0.10 \pm 0.38$ Mm⁻¹, respectively. Although both applications show a modal value close to 0.0 Mm⁻¹ and small standard deviation, the

in-flight values are characterized by a broader distribution compared to the laboratory values (Figure 6).

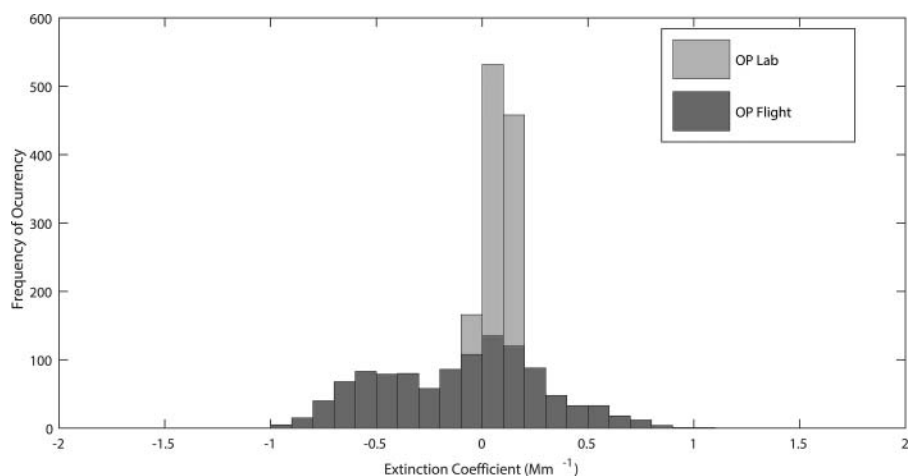
The cause for the broader distribution in flight could be that at laboratory conditions the instrument was operated with particle-free air while during flight at least a few particles were present. Regarding the limit of detection (3σ), there is an increase of the value in comparison to the laboratory results to values from 0.90, 0.45, and 0.20 Mm⁻¹ for 1, 10, and 60s averaging time, respectively, to 1.80, 1.14, and 0.90 Mm⁻¹. The typical lower aerosol extinction coefficients observed in the free troposphere range from 1 to 10 Mm⁻¹, which can be achieved by averaging over a period of 60 seconds for the lower limit.

We observed some negative extinction coefficient values during ascending/descending maneuvers of the aircraft during baseline measurements. These values were disregarded from the data analysis since we determine aerosol optical properties only from stable flight operation conditions. The solution for this problem will be addressed in upcoming work.

Characterization of different aerosol types

The CAPS PM_{ex}, together with OPC and CPC instruments, were operated simultaneously on board the research aircraft. The measurements performed by these instruments demonstrate the potential information to be provided by this kind of IAGOS prototype instrument. Although the CPC will not be part of the future IAGOS aerosol instruments containing the CAPS PM_{ex} and the OPC, the data will be used to further evaluate the results and potential capabilities of the instrument prototype.

For this purpose, the complete flight on 30th August from Bornholm (Denmark) across the Baltic Sea to Lindenberg (Germany) and further over Germany to Bremerhaven (Germany), the home base of the aircraft, was

**Figure 6.** Histogram of measured values of the laboratory tests and operation during flight (10s integration time).

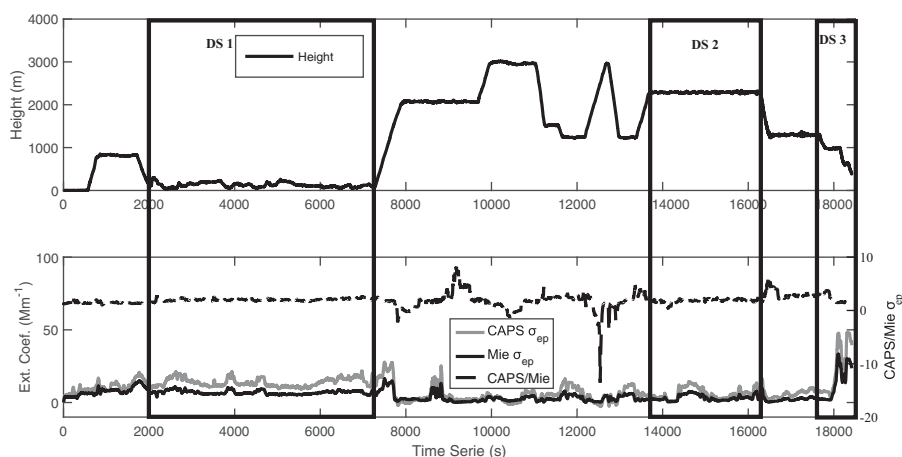


Figure 7. Sampling height, measured and calculated extinction coefficients σ_{ep} , and their ratio.

divided into separate datasets according to altitude and aerosol type. Three selected cases or datasets (DS) are marked in Figure 7 as parts of the time series of the entire flight. For each DS, the following parameters were investigated: air mass origin (maritime or continental), average and standard deviation of the calculated σ_{ep} , average and standard deviation of the measured σ_{ep} from the OPC size distribution using Mie theory, contribution of sub- μm and super- μm sized particles to the extinction coefficient, linear regression analysis between the measured and calculated extinction coefficients, number concentration of particles between 0.25 and 3 μm (OPC), and number concentration of particles below 0.25 μm (CPC minus OPC); all values are compiled in Table 3.

From the results shown in Table 3, Figure 7, Figure 8, and Figure 9, it is possible to demonstrate the potential of the IAGOS instrument prototype to characterize the aerosol type with respect to the optical properties and fractions of sub- μm and super- μm aerosol. The linear regression analysis of measured and calculated σ_{ep} shows a high correlation for all datasets with $R^2 \geq 0.74$, which is

expected since the Mie calculation (sizing channels are based on PSL sphere calibration and the refractive index of 1.59 for PSL is used) is based on the particles detected by the OPC which covers the optically relevant size range. The variation on the slope of the regression line between 0.39 and 0.67 is, most likely, associated with the presence of optically active particles below 250 nm in diameter which are not detectable by the OPC. Some fraction of the missing calculated extinction may be due to small absorbing black carbon containing particles not measured by the OPC or accounted for in the Mie calculations.

The lowest slope was found for DS 1, which is the dataset of the ship plume chasing. In this case, the aerosol number concentration is dominated by small particles. Nevertheless, DS1 also shows the highest σ_{ep} value for super- μm aerosol and the highest fraction of $\sigma_{ep, \text{super-}\mu\text{m}}/\sigma_{ep}$ of 5%, caused by marine aerosol particles. For DS 3, taken during the descent into Bremerhaven airport, the aerosol is dominated by urban pollution. Hence the extinction coefficient is the highest but the fraction of $\sigma_{ep, \text{super-}\mu\text{m}}/\sigma_{ep}$ of 1% is the lowest for the three data sets. For DS 3, the baseline was obtained

Table 3. (a) Flight datasets results from instruments. (b) Linear regression analysis results between the measured values and Mie Theory ($y = ax + b$).

3(a)								
DS	Env. Type	Avg. \pm Std σ_{ep} (CAPS) (Mm^{-1})	Avg. \pm Std σ_{ep} (Mie) (Mm^{-1})	Ratio σ_{ep} CAPS /Mie (Mm^{-1})	Avg. \pm Std σ_{ep} (sub- μm) (Mm^{-1})	Avg. \pm Std σ_{ep} (super- μm) (Mm^{-1})	Avg. \pm Std OPC ($\#/\text{cm}^3$)	Avg. \pm Std $d_p < 250$ nm ($\#/\text{cm}^3$) $\times 10^3$
DS1	Maritime	13.9 ± 2.9	7.0 ± 1.4	2.0 ± 0.2	13.0 ± 2.8	0.7 ± 0.2	67 ± 12	3.4 ± 2.6
DS2	Continental	6.5 ± 3.7	3.4 ± 2.3	1.9 ± 0.5	6.3 ± 3.6	0.2 ± 0.2	34 ± 20	1.4 ± 0.5
DS3	Continental	27.1 ± 15.7	17.2 ± 10.6	1.8 ± 0.6	26.8 ± 15.5	0.3 ± 0.2	173 ± 107	3.7 ± 1.7

3(b)						
DS	a	Std a	b	Std b	R^2	n
DS1	0.39	0.003	1.60	0.04	0.74	5221
DS2	0.54	0.002	0.04	0.02	0.96	2601
DS3	0.67	0.003	-0.95	0.10	0.99	610

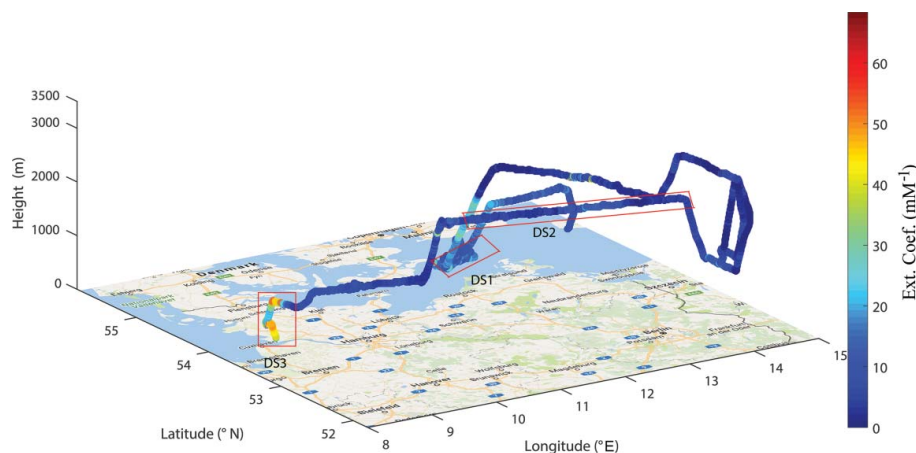


Figure 8. 3D plot of the altitude and extinction coefficient intensity throughout the complete flight and geographical location of the datasets.

before the beginning of the descent at stable pressure conditions. While other vertical motions exhibited (positive/negative) artifacts (see Figure 7) in the ratio of the measured-to-calculated extinction coefficients due to rapidly changing conditions, DS 3 did not exhibit these artifacts. The positive offset observed in DS 1 may be due to a baseline issue and needs to be further studied

From the partitioning of the total extinction into sub- μm and super- μm aerosols contributions, it can be seen that although the whole flight was characterized by a predominant fine-mode aerosol extinction coefficient, the highest contribution of coarse-mode (super- μm) aerosol is seen for the maritime environment at low altitude (between 0 and 1500 m), which is expected for such conditions and proves the potential of the set-up to provide such analysis.

Figure 8 shows the 3D vertical profile of the aerosol extinction measurement over the flight route. The high

resolution vertical and geographical extinction profile, together with the information on size distribution given by the OPC, provides very valuable information about aerosol characteristics, including the contribution of sub- μm and super- μm aerosol to the total extinction coefficient. Given the routine deployment of such an instrument within IAGOS, this high resolution data will also be used to validate remote sensing networks (such as ACTRIS and AERONET) and space-borne AOD observations, and together with other available measurement methods, such as the remote sensing technologies themselves, help better understanding the role played by aerosols in the Earth's climate system.

Summary and outlook

The original CAPS PM_{ex} instrument (Massoli et al. 2010) was modified for operation at reduced pressure levels

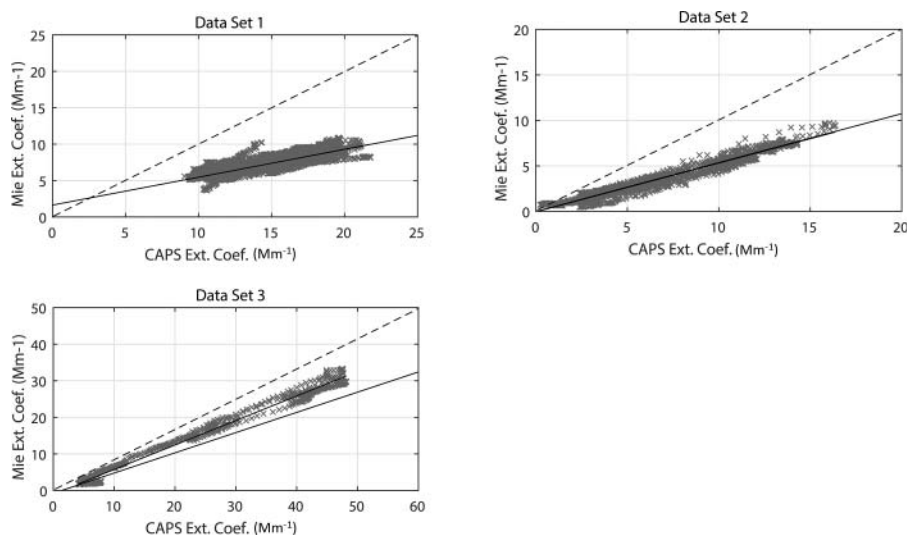


Figure 9. Correlation plot of the measured versus calculated by Mie theory extinction coefficients.

and under changing environmental conditions with respect to pressure and temperature, typical for operation aboard aircraft. These conditions are accounted for under normal baseline operations. Operation aboard aircraft, however, requires different handling of baseline operations. Instrument modifications were twofold. First, the flow system was equipped with mass flow controllers to maintain constant flows through the instrument for different pressure levels. An Allan variance analysis showed that the instrument noise at all pressure levels is in very good agreement to what has been found for ground-based operations (no pressure dependence) and that the resulting limit of detection of 0.2 Mm^{-1} for 60 seconds integration time is sufficient for measurements in the extratropical upper troposphere. Second, a temperature stabilization system was installed to minimize the observed influence of the instrument temperature on the signal.

Laboratory tests with particle-free air and CO_2 yield close agreement between measured extinction coefficients of the gases and data from literature, with a difference between 1 and 8% for both gases. More specifically, the measured extinction coefficients matched the expected extinction coefficients calculated for the different pressures and temperature conditions. The residual analysis showed that the residual values do not change with decreasing pressure. Residual values are in the order of $\pm 0.5 \text{ Mm}^{-1}$ for 1 second integration time and $\pm 0.2 \text{ Mm}^{-1}$ for 60 seconds integration time, throughout the complete pressure range studied. This finding underpins the conclusion that the CAPS PM_{ex} technology is operational down to 200 hPa for laboratory conditions.

During the in-flight tests, the system operated as expected and showed very promising results. Although it is not possible to compare the measured extinction coefficient values directly to some reference values, since no other instrument capable of measuring aerosol extinction was on board, the indirect comparison with extinction coefficients calculated from the measured size distribution by assuming Mie theory presented good agreement. The in-flight background noise of the instrument was not directly measured but deduced from a flight sequence in very clean air masses concerning optically active particles. Obtained in-flight background extinction coefficients scatter around 0.0 Mm^{-1} as for laboratory tests, but with a larger variability.

The following future modifications for a more robust measurement of aerosol extinction coefficients are suggested by this study: (a) a humidity sensor should be installed in the sample inlet to provide the precise characterization of the measured σ_{ep} variability and for comparison e.g. with LIDAR observations and (b) baseline timing and handling has to be improved for in-flight

operation, especially during vertical motions with rapidly changing temperature and pressure conditions.

The measurements during the in-flight test provided a data set for particle number concentration and size from the OPC and the aerosol light extinction coefficient from the CAPS PM_{ex} in accordance to what is expected for the sampled air masses. The tests successfully demonstrated that the IAGOS instrument prototype is able to provide rapid, in situ measurements of the extinction coefficient and the particle size distributions, and further characteristics, such as sub- μm and super- μm aerosol contributions to the total extinction coefficient, however, within the boundaries set by the deployed aerosol inlet system. These combined capabilities of the novel IAGOS instrument prototype will allow in the future to characterize aerosol types on the basis of optical properties and size, and to validate both remote sensing technologies and models.

For IAGOS operation a 60 sec integration time represents a spatial average of about 12 km along the flight track. In the UT/LS region this is sufficient as long as particle sources are remote. This is always the case if low particle (background) concentrations are observed. In this case the enhanced lower detection limit of the 60 sec average is needed. In case of local events and/or high concentrations a high spatial (200 m) resolution analysis of the events are possible because the 1 Hz data are stored regularly. A peak analysis of the 1 Hz data to identify these events is planned for IAGOS operations.

Acknowledgments

Parts of this work was funded by the EU FP7 project IGAS (Grant Agreement No. 312311), the Federal Ministry of Education and Research, Germany, in IAGOS-D (Grant Agreement No. 01LK1301A), EU H2020 Project ENVRIplus (Grant No. 654182) and HITEC Graduate School for Energy and Climate. The authors gratefully acknowledge valuable contributions from the Sea-Ice Physics group from Alfred-Wegener-Institute for giving us the opportunity to join the campaign BALTEX 2015.

ORCID

Julia Perim de Faria  <http://orcid.org/0000-0002-2280-2616>
 Ulrich Bundke  <http://orcid.org/0000-0001-5484-8099>
 Andrew Freedman  <http://orcid.org/0000-0002-5598-6626>
 Timothy B. Onasch  <http://orcid.org/0000-0001-7796-7840>
 Andreas Petzold  <http://orcid.org/0000-0002-2504-1680>

References

Anderson, T. L., Charlson, R. J., Bellouin, N., Boucher, O., Chin, M., Christopher, S. A., Haywood, J., Kaufman, Y. J., Kinne, S., Ogren, J. A., Remer, L. A., Takemura, T., Tanre,

- D., Torres, O., Trepte, C. R., Wielicki, B. A., Winker, D. M., and Yu, H. B. (2005). An “A-Train” Strategy for Quantifying Direct Climate Forcing by Anthropogenic Aerosols. *Bull. Amer. Meteorol. Soci.*, 86:1795–1809.
- Anderson, T. L., Covert, D. S., Marshall, S. F., Laucks, M. L., Charlson, R. J., Waggoner, A. P., Ogren, J. A., Caldwell, R., Holm, R. L., Quant, F. R., Sem, G. J., Wiedensohler, A., Ahlquist, N. A., and Bates, T. S. (1996). Performance Characteristics of a High-Sensitivity, Three-Wavelength, Total Scatter/Backscatter Nephelometer. *J. Atmos. Oceanic Technol.*, 13:967–986.
- Bodhaine, B. A., Ahlquist, N. C., and Schnell, R. C. (1991). 3-Wavelength Nephelometer Suitable for Aircraft Measurement of Background Aerosol Scattering Coefficient. *Atmos. Environ. Part a-General Topics.*, 25:2267–2276.
- Bodhaine, B. A., Wood, N. B., Dutton, E. G., and Slusser, J. R. (1999). On Rayleigh Optical Depth Calculations. *J. Atmos. Oceanic Technol.*, 16:1854–1861.
- Bojinski, S., Verstraete, M., Peterson, T. C., Richter, C., Simmons, A., and Zemp, M. (2014). The Concept of Essential Climate Variables in Support of Climate Research, Applications, and Policy. *Bull. Amer. Meteorol. Soc.*, 95:1431–1443.
- Boucher, O., Randall, D., Artaxo, P., Bretherton, C., Feingold, G., Forster, P., Kerminen, V.-M., Kondo, Y., Liao, H., Lohmann, U., Rasch, P., Satheesh, S. K., Sherwood, S., Stevens, B., and Zhang, X. Y. (2013). Clouds and Aerosols, in Climate Change 2013: The Physical Science Basis. *Contribution of Working Group I to the Fifth Assessment Report of the Intergovernmental Panel on Climate Change*, T. F. Stocker, D. Qin, G.-K. Plattner, M. Tignor, S. K. Allen, J. Boschung, A. Nauels, Y. Xia, V. Bex, P. M. Midgley, eds., Cambridge University Press, Cambridge, United Kingdom and New York, NY, USA, pp. 571–658.
- Bundke, U., Berg, M., Ibrahim, A., Tettich, F., Klaus, C., Franke, H., Fiebig, M., and Petzold, A. (2015). The IAGOS-CORE Aerosol Package: Instrument Design, Operation and Performance for Continuous Measurement Aboard in-Service Aircraft. *Tellus Ser. B-Chem. Phys. Meteorol.*, 67:28339.
- Cutten, D. R. (1974). Rayleigh-Scattering Coefficients for Dry Air, Carbon-Dioxide, and Freon-12. *Appl. Opt.*, 13:468–469.
- Haywood, J. M., and Shine, K. P. (1995). The Effect of Anthropogenic Sulfate and Soot Aerosol on the Clear-Sky Planetary Radiation Budget. *Geophys. Res. Lett.*, 22:603–606.
- Holben, B. N., Eck, T. F., Slutsker, I., Tanre, D., Buis, J. P., Setzer, A., Vermote, E., Reagan, J. A., Kaufman, Y. J., Nakajima, T., Lavenu, F., Jankowiak, I., and Smirnov, A. (1998). AERONET – A Federated Instrument Network and Data Archive for Aerosol Characterization. *Remote Sens. Environ.*, 66:1–16.
- Holben, B. N., Tanre, D., Smirnov, A., Eck, T. F., Slutsker, I., Abuhassan, N., Newcomb, W. W., Schafer, J. S., Chatenet, B., Lavenu, F., Kaufman, Y. J., Castle, J. V., Setzer, A., Markham, B., Clark, D., Frouin, R., Halthore, R., Karneli, A., O’Neill, N. T., Pietras, C., Pinker, R. T., Voss, K., and Zibordi, G. (2001). An Emerging Ground-Based Aerosol Climatology: Aerosol Optical Depth from AERONET. *J. Geophys. Res.*, 106:12067–12097.
- Kebabian, P. L., Robinson, W. A., and Freedman, A. (2007). Optical Extinction Monitor using cw Cavity Enhanced Detection. *Rev. Sci. Instrument.*, 78:063102.
- Massoli, P., Kebabian, P. L., Onasch, T. B., Hills, F. B., and Freedman, A. (2010). Aerosol Light Extinction Measurements by Cavity Attenuated Phase Shift (CAPS) Spectroscopy: Laboratory Validation and Field Deployment of a Compact Aerosol Particle Extinction Monitor. *Aerosol Sci. Tech.*, 44:428–435.
- McComiskey, A., Schwartz, S. E., Schmid, B., Guan, H., Lewis, E. R., Ricchiuzzi, P., and Ogren, J. A. (2008). Direct Aerosol Forcing: Calculation from Observables and Sensitivities to Inputs. *J. Geophys. Res.-Atmos.*, 113:D09202.
- Moosmüller, H., Varma, R., and Arnott, W. P. (2005). Cavity Ring-Down and Cavity-Enhanced Detection Techniques for the Measurement of Aerosol Extinction. *Aerosol Sci. Technol.*, 39:30–39.
- Mylre, G., Shindell, D., Bréon, F.-M., Collins, W., Fuglestedt, J., Huang, J., Koch, D., Lamarque, J.-F., Lee, D., Mendoza, B., Nakajima, T., Robock, A., Stephens, G., Takemura, T., and Zhang, H. (2013). Anthropogenic and Natural Radiative Forcing, in Climate Change 2013: The Physical Science Basis. *Contribution of Working Group I to the Fifth Assessment Report of the Intergovernmental Panel on Climate Change*, T. F. Stocker, D. Qin, G.-K. Plattner, M. Tignor, S. K. Allen, J. Boschung, A. Nauels, Y. Xia, V. Bex, P. M. Midgley, eds., Cambridge University Press, Cambridge, United Kingdom and New York, NY, USA, 659–740.
- Pappalardo, G., Amodeo, A., Apituley, A., Comeron, A., Freudenthaler, V., Linne, H., Ansmann, A., Bosenberg, J., D’Amico, G., Mattis, I., Mona, L., Wandinger, U., Amiridis, V., Alados-Arboledas, L., Nicolae, D., and Wiegner, M. (2014). EARLINET: Towards an Advanced Sustainable European Aerosol Lidar Network. *Atmos. Meas. Tech.*, 7:2389–2409.
- Petzold, A., Fiebig, M., Flentje, H., Keil, A., Leiterer, U., Schröder, F., Stifter, A., Wendisch, M., Wendling, P. (2002). Vertical Variability of Aerosol Properties Observed at a Continental Site During the Lindenberg Aerosol Characterization Experiment (LACE 98). *J. Geophys. Res.: Atmos.*, 107(D21):8128.
- Petzold, A., Formenti, P., Baumgardner, D., Bundke, U., Coe, H., Curtius, J., DeMott, P. J., Flagan, R. C., Fiebig, M., Hudson, J. G., McQuaid, J., Minikin, A., Roberts, G. C., and Wang, J. (2013a). *In Situ Measurements of Aerosol Particles, in Airborne Measurements for Environmental Research*, M. Wendisch and J. L. Brenguier, eds., Wiley-VCH Verlag GmbH & Co. KGaA, Weinheim, pp. 157–223.
- Petzold, A., Onasch, T., Kebabian, P., Freedman, A. (2013b). Intercomparison of a Cavity Attenuated Phase Shift-Based Extinction Monitor (CAPS PMex) with an Integrating Nephelometer and a Filter-Based Absorption Monitor. *Atmos. Meas. Tech.*, 6:1141–1151.
- Petzold, A., Thouret, V., Gerbig, C., Zahn, A., Brenninkmeijer, C. A. M., Gallagher, M., Hermann, M., Pontaud, M., Ziereis, H., Boulanger, D., Marshall, J., Nédélec, P., Smit, H. G. J., Frieß, U., Flaud, J.-M., Wahner, A., Cammas, J.-P., Volz-Thomas, A., IAGOS-Team. (2015). Global-Scale Atmosphere Monitoring by In-Service Aircraft – Current Achievements and Future Prospects of the European Research Infrastructure IAGOS. *Tellus Ser. B-Chem. Phys. Meteorol.*, 67:28452.
- Schmid, B., Ferrare, R., Flynn, C., Elleman, R., Covert, D., Strawa, A., Welton, E., Turner, D., Jonsson, H., Redemann, J., Eilers, J., Ricci, K., Hallar, A. G., Clayton, M., Michalsky, J., Smirnov, A., Holben, B., and Barnard, J. (2006). How well do State-of-the-Art Techniques Measuring the Vertical Profile of Tropospheric Aerosol Extinction Compare? *J. Geophys. Res.-Atmos.*, 111:D05S07.

- Sheridan, P. J., Andrews, E., Ogren, J. A., Tackett, J. L., and Winker, D. M. (2012). Vertical Profiles of Aerosol Optical Properties Over Central Illinois and Comparison with Surface and Satellite Measurements. *Atmos. Chem. Phys.*, 12:11695–11721.
- Sneep, M., and Ubachs, W. (2005). Direct Measurement of the Rayleigh Scattering Cross Section in Various Gases. *J. Quant. Spectros. Radiat. Transfer.*, 92:293–310.
- Strawa, A. W., Castaneda, R., Owano, T., Baer, D. S., Paldus, B. A. (2003). The Measurement of Aerosol Optical Properties using Continuous Wave Cavity Ring-Down Techniques. *J. Atmos. Ocean. Tech.*, 20:454–465.
- Thalman, R., Zarzana, K. J., Tolbert, M. A., and Volkamer, R. (2014). Rayleigh Scattering Cross-Section Measurements of Nitrogen, Argon, Oxygen and Air. *J. Quant. Spectros. Radiat. Transf.*, 147:171–177.
- Weinzierl, B., Petzold, A., Esselborn, M., Wirth, M., Rasp, K., Kandler, K., Schütz, L., Koepke, P., and Fiebig, M. (2009). Airborne Measurements of Dust Layer Properties, Particle Size Distribution and Mixing State of Saharan Dust During SAMUM 2006. *Tellus.* 61B:96–117.
- Yu, Z. H., Ziemba, L. D., Onasch, T. B., Herndon, S. C., Albo, S. E., Miake-Lye, R., Anderson, B. E., Keabian, P. L., and Freedman, A. (2011). Direct Measurement of Aircraft Engine Soot Emissions Using a Cavity-Attenuated Phase Shift (CAPS)-Based Extinction Monitor. *Aerosol Sci. Technol.*, 45:1319–1325.